The AAPS Journal, Vol. 10, No. 1, March 2008 (© 2007)
DOI: 10.1208/s12248-007-9001-8

Research Article

Pharmacokinetic Interaction between the Flavonoid Luteolin and γ-Hydroxybutyrate in Rats: Potential Involvement of Monocarboxylate Transporters

Xiaodong Wang,[1] Qi Wang,[2] and Marilyn E. Morris[1,3]

Received 17 October 2007; accepted 10 December 2007; published online 30 January 2008

Abstract. Monocarboxylate transporter 1 (MCT1) has been previously reported as an important determinant of the renal reabsorption of the drug of abuse, γ-hydroxybutyrate (GHB). Luteolin is a potent MCT1 inhibitor, inhibiting the uptake of GHB with an IC_{50} of 0.41 μM in MCT1-transfected MDA-MB231 cells. The objectives of this study were to characterize the effects of luteolin on GHB pharmacokinetics and pharmacodynamics in rats, and to investigate the mechanism of the interaction using model-fitting methods. GHB (400 and 1,000 mg/kg) and luteolin (0, 4 and 10 mg/kg) were administered to rats via iv bolus doses. The plasma or urine concentrations of luteolin and GHB were determined by HPLC and LC/MS/MS, respectively. The pharmacodynamic parameter sleep time in rats after GHB administration was recorded. A pharmacokinetic model containing capacity-limited renal reabsorption and metabolic clearance was constructed to characterize the *in vivo* interaction. Luteolin significantly decreased the plasma concentration and AUC, and increased the total and renal clearances of GHB. Moreover, luteolin significantly shortened the duration of GHB (1,000 mg/kg)-induced sleep in rats (161 ± 16, 131 ± 14 and 121 ± 5 min for control, luteolin 4 and 10 mg/kg groups, respectively, $p < 0.01$). An uncompetitive inhibition model, with an inhibition constant of 1.1 μM, best described the *in vivo* pharmacokinetic interaction. The results of this study indicated that luteolin significantly altered the pharmacokinetics of GHB by inhibiting its MCT1-mediated transport. The interaction between luteolin and GHB may offer a potential clinical detoxification strategy to treat GHB overdoses.

KEY WORDS: γ-hydroxybutyrate; luteolin; MCT; pharmacokinetic interactions.

INTRODUCTION

Monocarboxylate transporters (MCTs), which belong to the solute carrier 16 (SLC 16) gene family, play an essential role in cellular metabolism (1). Of the now 14 identified MCT members, MCT 1–4 have been shown to be proton-coupled monocarboxylate transporters, important in the transport of endogenous monocarboxylates, such as pyruvate, lactate and ketone bodies (1,2), as well as clinically relevant drugs, such as foscarnet (3), nateglinide (4) and lovastatin (5). Among these four MCTs, MCT1 is expressed nearly ubiquitously throughout the body, including erythrocytes, muscle, heart, kidney, intestine, liver and brain (2). Transport of lactate by MCT1 across the plasma membrane to maintain cytosolic pH is physiologically important to mammalian cells under hypoxia conditions (1).

The typical inhibitors of MCT1 include 4, 4′-diisothiocyanostilbene-2, 2′-disulphonate (DIDS) and bulky monocarboxylates such as α-cyano-4-hydroxycinnamate (CHC) (1). Recently, we reported that flavonoids, a class of polyphenolic compounds present in the diet and herbal products, are potent MCT1 inhibitors as well. Among all the flavonoids tested, luteolin (3′,4′,5,7-tetrahydroxyflavone), a naturally occurring flavonoid abundant in vegetables (6) with reported anti-oxidant (7) and anti-inflammatory activities (8), represents one of the most potent inhibitors, with an IC_{50} of 0.41 μM in inhibiting the uptake of GHB in MCT1-transfected MDA-MB231 cells (9).

Recently, due to the popular use of dietary supplements and herbal medicines, flavonoid-drug interactions have increasingly been observed in preclinical and clinical studies (10, 11). These interactions, in some cases, can cause serious or life-threatening adverse effects, especially when flavonoids are used together with narrow therapeutic index drugs (12). On the other hand, flavonoids have been shown to be able to improve the bioavailability of the coadministered drugs, resulting in beneficial flavonoid-drug interactions (11,13). The mechanisms underlying these flavonoid-drug interactions are presumably due to the inhibition of drug metabolizing

Xiaodong Wang and Qi Wang contributed equally to this work.

[1] Department of Pharmaceutical Sciences, University at Buffalo, State University of New York, 517 Hochstetter Hall, Amherst, New York 14260, USA.
[2] *Present Address:* Bristol Myers Squibb, Mailstop HW17 1.07, 311 Pennington Rocky-Hill Rd, Pennington, New Jersey 08534, USA.
[3] To whom correspondence should be addressed. (e-mail: memorris@buffalo.edu)

enzymes and efflux drug transporters, such as P-glycoprotein (ABCB1) and Breast Cancer Resistance Protein (ABCG2) (11–13). However, far less information is available on flavonoid-drug interactions involving uptake transporters, including the monocarboxylate transporters.

The physiological substrates of MCT1 include pyruvate, lactate and ketone bodies (1). In recent studies, we demonstrated that MCT1 also represents an important transporter for γ-hydroxybutyrate (GHB) (14), a drug used to treat the sleep disorder narcolepsy (15). GHB is also a drug of abuse (16), and GHB abuse and subsequent overdoses may lead to serious adverse effects, such as coma, seizure, respiratory arrest and even death (17). Current treatment of GHB overdoses mainly consists of supportive care and no specific detoxification strategies have been developed for clinical use (17).

The pharmacokinetics of GHB are nonlinear in rats and humans, due to its capacity-limited metabolism (18–20), capacity-limited oral absorption (21,22), and capacity-limited renal clearance (20). At higher doses when the metabolic clearance is saturated, the renal clearance of GHB following intravenous administration becomes more pronounced and significantly contributes to the overall elimination of GHB (20). An important, if not the only mechanism underlying this capacity-limited renal clearance of GHB is the extensive renal reabsorption mediated by monocarboxylate transporters in the kidney proximal tubules (14,20). Given the potent inhibitory effects of luteolin on MCT1 and significant contribution of MCT1 in GHB renal reabsorption, it is very likely that a MCT1-mediated luteolin and GHB interaction might occur in vivo. In a previous preliminary study, we have demonstrated that luteolin (10 mg/kg, iv bolus) significantly decreased the plasma concentration of GHB, increased its renal clearance and shortened the duration of GHB-induced sleep in rats (9).

The objectives of this study were (1) to characterize the pharmacokinetic interaction between luteolin and GHB; (2) to construct a pharmacokinetic model for the interaction between luteolin and GHB, and use this model to explore the possible *in vivo* inhibition mechanism; and (3) to use our model to predict the pharmacokinetic consequences of MCT1-mediated drug-drug interactions.

MATERIALS AND METHODS

Chemicals and Reagents

Luteolin, apigenin, γ-hydroxybutyrate, hydroxypropyl-β-cyclodextrin were purchased from Sigma-Aldrich (St. Louis, MO, USA). The internal standard GHB-D6 was purchased from Cerilliant (Round Rock, TX, USA). Saline was purchased from Henry-Schein (Melville, NY, USA). All other reagents or solvents used were either analytical or high-performance liquid chromatography (HPLC) grade.

Animals and Surgery

Male Sprague–Dawley (SD) rats (body weight ~ 300 g) were purchased from Harlan (Indianapolis, IN, USA). Animals were housed in a temperature and humidity-controlled environment with a 12-h light/dark cycle and received a standard diet with free access to tap water. Animals were acclimatized to this environment for at least one week before experiments. All protocols of animal studies were reviewed and approved by the University at Buffalo Institutional Animal Care and Use Committee. The rats had cannulas implanted in the right jugular vein and bladder under anesthesia (ketamine 90 mg/kg and xylazine 10 mg/kg, im injection) as previously described (20), and were kept in individual cages for recovery from surgery for three days.

Pharmacokinetic Studies

Pharmacokinetic studies were performed as previously reported (9). The rats were kept in metabolic cages for blood and urine collection throughout the study. GHB was dissolved in sterile water as a 200 mg/ml solution and was given to rats via an iv bolus injection for specified doses. Luteolin was dissolved in dimethyl sulfoxide (DMSO) as a 50 mg/ml stock solution and was further diluted with hydroxypropyl-β-cyclodextrin (25%) to such concentrations that specified doses were delivered as 2 μl/g body weight drug solution. The luteolin solution was injected intravenously right after the GHB injection. For the control group, GHB (400 or 1,000 mg/kg) and the luteolin control vehicle were given to rats. For the luteolin treatment group, GHB (400 or 1,000 mg/kg) and luteolin (4 or 10 mg/kg) were administered to rats. Blood samples (200 μl) were collected from the jugular vein cannula at 0 (predose), 2, 5, 10, 30, 60, 120, 150, 180, 210, 240, and 300 min after GHB administration. The plasma was separated from the whole blood by centrifugation at 2,000 g for 5 min at 4°C. The urine samples were collected over 6 h and the volume was measured. All plasma and urine samples were stored at −80°C until analysis. The hypnotic effects of GHB following various treatments were determined by the sleep time, which was measured as the difference in the time between the loss of righting reflex (LRR) and return of righting reflex (RRR).

HPLC and LC/MS/MS Assay

The concentration of luteolin in plasma samples was determined by a previously published method with minor modifications (23,24). Briefly, 100 μl of 6.0% perchloric acid was added to 100 μl plasma sample to precipitate protein. Ten microliter of apigenin solution (100 μg/ml) was added as the internal standard. Luteolin was extracted by adding 1.5 ml of ethyl acetate followed by vigorous vortexing. The mixture was centrifuged at 2,000 g for 10 min. The supernatant was transferred to a new tube and dried under a stream of nitrogen. The residue was reconstituted in 100 μl of mobile phase followed by centrifugation at 22,000×*g* for 10 min and 60 μl of supernatant was injected into the HPLC for analysis.

The HPLC analysis was performed on a system consisting of a Waters 1525 pump, a Waters Breeze™ workstation, 717 plus autosampler, a 2847 UV detector, and an Alltech Alltima C_{18} column (125×4.6 mm, 5-μm particle size). The composition of the mobile phase was methanol/0.2% phosphoric acid solution (60:40, *v*/*v*). The mobile phase was delivered isocratically with a flow rate of 1.0 ml/min. UV absorbance was measured at 350 nm. Luteolin appeared on the chromatograph at approximately 7 min with no interfering peaks. The standard curve was linear over the concentra-

tion range of 0.01 to 20 μg/ml with a regression coefficient greater than 0.99. The lower limit of quantitation of luteolin was 10 ng/ml.

The concentration of GHB in plasma and urine samples was determined by a validated liquid chromatography-tandem mass spectrometry (LC/MS/MS) assay as previous described with minor modifications (9,25). Briefly, to generate a calibration curve, a GHB-D6 stock solution (6 mM, 5 μl) and GHB stock solutions with varying concentrations were added into blank plasma or urine (50 μl; appropriately diluted with water) in order to prepare standards of GHB (60, 240, 600, 1,200, 2,400, 4,800, and 7,200 μM as final concentrations). To each plasma or urine sample, the internal standard GHB-D6 was added in the same concentration and volume. The protein present in plasma and urine samples was precipitated with methanol (1 vol of methanol added to 1 vol sample). After vigorous vortexing, the mixtures were centrifuged at 22,000×*g* for 20 min, the supernatant was collected for LC/MS/MS assay.

The LC/MS/MS assay of GHB was performed on a PE SCIEX API 3000 triple-quadruple tandem mass spectrometer system equipped with a turbo ion spray (Applied Biosystems, Foster City, CA, USA), a Series 200 PE autosampler (Perkin–Elmer, Shelton, CT), and a Series 200 PE micro pump (Perkin–Elmer). The sample separation by liquid chromatography was conducted using a reversed-phase Aqua C_{18} 5 μm 125 Å column (150×4.6 mm, Phenomenex, Torrance, CA, USA) connected with a C_{18} 5 μm guard column cartridge system (Phenomenex). The mobile phase consisting of 5 mM formic acid/methanol (33:67, *v*/*v*) was delivered isocratically. The flow rate was 0.75 ml/min and the injection volume was 10 μl. The actual flow into the mass-spectrum was achieved by using a splitter, which accounted for one third of total flow. The turbo ion spray was operated in the positive mode with interface temperature set at 400°C. The declustering potential and collision energy for fragmentation was set at 30 and 13 eV, respectively. Multiple reaction monitoring was applied to detect GHB-D6 and GHB by measuring the ion pair transitions from *m*/*z* 111 (parent ion) to *m*/z 93 (product ion) and from *m*/*z* 105 (parent ion) to *m*/*z* 87 (product ion), respectively. The retention time of GHB-D6 and GHB was 2.6 min with no interfering peaks found in plasma and urine samples. The Analyst software 1.4.1 (Applied Biosystems, Foster City, CA, USA) was used for data quantitation and instrument control.

Pharmacokinetic Assessment

The total clearance of GHB (CL) was determined from Dose/AUC, where AUC is the area under the plasma concentration-time curve. Renal clearance (CL_R) was determined by A_e/AUC, where A_e is the amount of GHB excreted into the urine. The fraction of the dose eliminated by renal excretion (f_e) was determined by A_e/Dose. The metabolic clearance (CL_m) was calculated using the equation $CL_m = CL - CL_R$, assuming that total clearance of GHB is equal to renal clearance plus metabolic clearance.

To better understand the *in vivo* interaction between luteolin and GHB, pharmacokinetic modeling was conducted to characterize both luteolin and GHB kinetics. First of all, luteolin data were fitted with different pharmacokinetic models, e.g. one-compartment, two-compartment and three-compartment models with linear or nonlinear elimination. The final pharmacokinetic model for luteolin (Eqs. 1 and 2) was selected based on the goodness-of-fit criteria including coefficient variation of the estimates (CV %), R^2, Akaike's Information Criterion (AIC) and Schwarz Criterion (SC) by using ADAPTII software (BMSR, University of South California, Los Angeles CA).

$$\frac{dX_{C\_Lut}}{dt} = -k_{10} \cdot X_{C\_Lut} - k_{12} \cdot X_{C\_Lut} + k_{21} \times X_{T\_Lut}(IC = Dose) \quad (1)$$

$$\frac{dX_{T\_Lut}}{dt} = k_{12} \cdot X_{C\_Lut} - k_{21} \cdot X_{T\_Lut}(\mathrm{IC} = 0) \quad (2)$$

where X_{C_Lut} and X_{T_Lut} represents the luteolin amount in the central and peripheral compartment, respectively. k_{10} represents the elimination rate constant of the central compartment. k_{12} and k_{21} represent the first-order rate constants of distribution between the two compartments. The initial condition for each equation is shown in parenthesis.

The pharmacokinetics of GHB has previously been characterized by a one-compartment nonlinear model (19). The nonlinearity in GHB kinetics, following intravenous administration, is related to the capacity-limited metabolism (18–20) and capacity-limited renal reabsorption (20). Therefore, a one-compartment model was used to describe the GHB pharmacokinetics with the incorporation of capacity-limited metabolism, glomerular filtration, and capacity-limited reabsorption, as shown in Eq. 3 and Fig. 4. In this model, several assumptions were made: (1) no or minimal effects of luteolin on GHB metabolism; (2) no or minimal renal secretion of GHB; and (3) only parent luteolin inhibits MCT1. To our knowledge, there is no report in the literature of luteolin affecting the metabolism of GHB. The negligible renal secretion of GHB was assumed based on a previous study, in which a lack of renal secretion was reported for the ketone bodies of β-hydroxybutyrate or the congener of GHB with the hydroxyl group at carbon 3 (26). We also assumed only parent luteolin could inhibit MCT1 since flavonoid glycosides were reported previously with no or minimal MCT1 inhibitory activity (9).

The Eq. 3 describes the pharmacokinetics of GHB in the absence of luteolin, while Eq. 4 describes the pharmacokinetics of GHB in the presence of luteolin as a competitive inhibitor on GHB renal clearance. Eqs. 5 and 6 describe the pharmacokinetics of GHB in the presence of luteolin as a noncompetitive and uncompetitive inhibitor on GHB renal clearance, respectively. Simultaneous fitting was conducted based on the integrated luteolin model and GHB model to evaluate the *in vivo* inhibition mechanism. The final pharmacokinetic model for luteolin and GHB was selected based on the goodness-of-fit criteria (CV % of the estimates, R^2, AIC and SC) by using ADAPTII software.

$$\frac{dX_{GHB}}{dt} = -\frac{V_{\max} \cdot X_{GHB}}{k_m \cdot V_{GHB} + X_{GHB}} - \left(\frac{GFR}{V_{GHB}} - \frac{V_{max\_ren}}{k_{ren} \cdot V_{GHB} + X_{GHB}}\right) \times X_{GHB}(IC = Dose) \quad (3)$$

$$\frac{dX_{\mathrm{GHB}}}{dt} = -\frac{V_{\max}\cdot X_{GHB}}{k_m\cdot V_{GHB}+X_{GHB}} - \left(\frac{GFR}{V_{\mathrm{GHB}}} - \frac{V_{\max\_\mathrm{ren}}}{k_{\mathrm{ren}}\cdot V_{\mathrm{GHB}}\cdot\left(1+\frac{I}{K_i}\right)+X_{\mathrm{GHB}}}\right) \times X_{\mathrm{GHB}}(\mathrm{IC}=\mathrm{Dose}) \quad (4)$$

$$\frac{\mathrm{d}X_{\mathrm{GHB}}}{\mathrm{d}t} = -\frac{V_{\max}\cdot X_{\mathrm{GHB}}}{k_{\mathrm{m}}\cdot V_{\mathrm{GHB}}+X_{\mathrm{GHB}}} - \left(\frac{\mathrm{GFR}}{V_{\mathrm{GHB}}} - \frac{V_{\max\_\mathrm{ren}}\Big/\left(1+\frac{I}{K_i}\right)}{k_{\mathrm{ren}}\cdot V_{\mathrm{GHB}}+X_{\mathrm{GHB}}}\right) \times X_{\mathrm{GHB}}(\mathrm{IC}=\mathrm{Dose}) \quad (5)$$

$$\frac{\mathrm{d}X_{\mathrm{GHB}}}{\mathrm{d}t} = -\frac{V_{\max}\cdot X_{\mathrm{GHB}}}{k_{\mathrm{m}}\cdot V_{\mathrm{GHB}}+X_{\mathrm{GHB}}} - \left(\frac{\mathrm{GFR}}{V_{\mathrm{GHB}}} - \frac{V_{\max\_\mathrm{ren}}\Big/\left(1+\frac{I}{K_i}\right)}{k_{\mathrm{ren}}\cdot V_{\mathrm{GHB}}\Big/\left(1+\frac{I}{K_i}\right)+X_{\mathrm{GHB}}}\right) \times X_{\mathrm{GHB}}(\mathrm{IC}=\mathrm{Dose}) \quad (6)$$

where X_{GHB} represents the GHB amount in the central compartment. V_{GHB} represents the volume of distribution of GHB. $V_{\max}$ represents the maximal metabolic rate of GHB and k_{m} represents the concentration of GHB at 50% of $V_{\max}$. GFR represents the glomerular filtration rate in the kidney. $V_{\max\_\mathrm{ren}}$ represents the maximal rate of GHB renal reabsorption and k_{ren} represents the concentration of GHB at 50% of the maximal reabsorption rate. I represents luteolin in the central compartment ($X_{\mathrm{C\_Lut}}$) that inhibits GHB reabsorption and K_{i} represents the inhibition constant at 50% of inhibition.

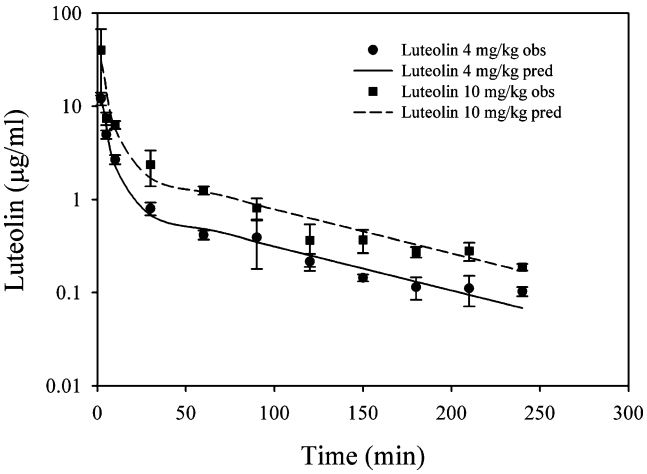

Fig. 1. Pharmacokinetics of luteolin in rats following intravenous administration. Plasma concentrations of luteolin at doses of 4 mg/kg (*filled circle*) and 10 mg/kg (*filled square*) are plotted as mean±SD, n=3 for both groups. The *solid* and *dashed lines* represent the fitted lines for the doses of 4 and 10 mg/kg, respectively. The model fitting results were obtained using Eqs. 1 and 2

To determine the effects of varying doses of luteolin on GHB detoxification at different dose levels of GHB, model simulations were conducted using the parameters obtained from the above nonlinear regression analysis with the incorporation of a 10% variance using ADAPT II software. Three doses of GHB (200, 400 and 1,000 mg/kg by iv bolus) and five doses of luteolin (0, 2, 4, 10, and 20 mg/kg by iv bolus) were simulated based on the proposed pharmacokinetic model.

Statistical Analysis

Data were analyzed for statistically significant differences using ANOVA (Prism 3.0 software, GraphPad, San Diego, CA, USA) followed by a Dunnett's post hoc test or by the Student's t test. p values<0.05 were considered statistically significant.

RESULTS

Pharmacokinetics of Luteolin

To characterize the interaction between luteolin and GHB, it is essential to determine the pharmacokinetics of luteolin. Therefore, we measured the plasma concentrations of luteolin over time following two iv doses. As shown in Fig. 1, after intravenous administration, luteolin plasma concentrations could be described by a biexponential equation, exhibiting a rapid decrease at the early time points followed by a slower decrease beyond 90 min, indicating the involvement of multiple compartment pharmacokinetics. Following doses of 4 and 10 mg/kg, the AUC of luteolin was 189±9 and 541±173 μg ml^{-1} min (mean±SD), respectively. The clearance of luteolin was similar at these two doses (21.2±1.1 and 19.7±5.5 ml min^{-1} kg^{-1} for the 4 and 10 mg/kg doses, respectively).

Effects of Luteolin on GHB Pharmacokinetics and Pharmacodynamics

To further investigate the *in vivo* MCT1-mediated interaction, GHB (400 or 1,000 mg/kg) and luteolin (0, 4 or 10 mg/kg) were administered to rats intravenously. As shown in Fig. 2, GHB plasma concentration versus time profiles exhibited nonlinear kinetics, which is consistent with previous reports (9, 19). When GHB was given at the dose of 1,000 mg/kg, luteolin effectively decreased the plasma concentrations of GHB. Compared with the GHB alone (control) group, the AUC of GHB was significantly decreased from 170±40 mg ml^{-1} min in the control rats to 117±29 mg ml^{-1} min (p<0.05) and 113±21 mg ml^{-1} min (p<0.05) for luteolin 4 and 10 mg/kg group, respectively (Table 1). In contrast, the total clearance of GHB was significantly increased from 6.19±1.59 ml min^{-1} kg^{-1} in the control group to 8.92±2.02 ml min^{-1} kg^{-1} (p<0.05) in the luteolin 4 mg/kg group and 9.05±1.43 ml min^{-1} kg^{-1} (p<0.05) in the luteolin 10 mg/kg group. Similarly, the renal clearance of GHB was significantly increased in the luteolin 10 mg/kg group when compared with the control group (p< 0.05, 1.64±0.62 and 3.84±1.21 ml min^{-1} kg^{-1} for the control and luteolin 10 mg/kg groups, respectively). However, the metabolic clearance of GHB was not significantly altered among the control and luteolin treatment groups. In addition to the effects of luteolin on GHB pharmacokinetics, luteolin

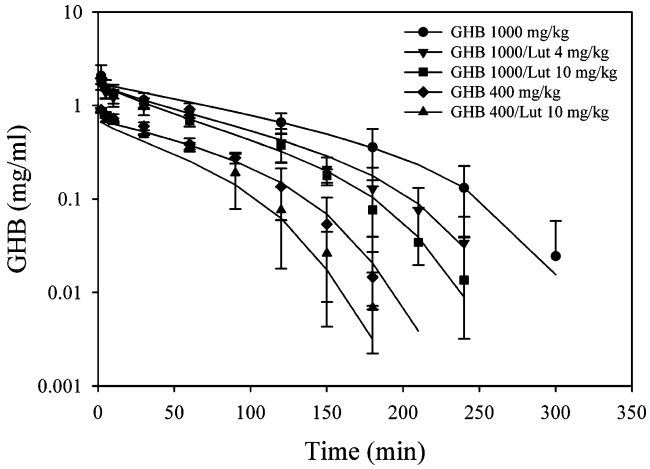

Fig. 2. Effects of luteolin on GHB pharmacokinetics in rats following intravenous coadministration. Plasma concentrations of GHB (1,000 mg/kg) in the absence (*filled circle*) or presence of luteolin at the doses of 4 mg/kg (*filled inverted triangle*) and 10 mg/kg (*filled square*) are plotted as mean±SD. Data points shown as (*filled diamond*) and (*filled triangle*) represent the plasma concentrations of GHB (400 mg/kg) in the absence or presence of luteolin (10 mg/kg), respectively. n=3-6 for each group. The *lines* represent the fitted lines obtained from the simultaneous fitting of the data using Eqs. 1, 2, 3 and 6

significantly shortened the duration of GHB-induced sleep in rats. Compared with the GHB only group, the total sleep time was decreased from 161±16 min in the control rats to 131±14 min (p<0.01) in the luteolin 4 mg/kg group and 121±5 min (p<0.01) in the luteolin 10 mg/kg group. At the lower dose of GHB (400 mg/kg), the AUC of GHB in control rats was 56.6±6.3 mg ml^{-1} min, which is similar to literature data (27). At this GHB dose level, similar effects of luteolin (10 mg/kg) on GHB pharmacokinetics and pharmacodynamics were observed (Table 1). However, the decrease in GHB AUC and increase in GHB total and renal clearances were less pronounced when compared with the changes at the higher dose of GHB. At the GHB dose of 400 mg/kg, the time for loss of righting reflex (onset of sleep) in rats was later (10±4 min) than that observed in the GHB 1000 mg/kg group (~2 min). Interestingly, luteolin (10 mg/kg) significantly delayed the onset of GHB (400 mg/kg)-induced sleep to 23±8 min (p<0.05, compared to 10±4 min), with no evident effects on the onset of GHB (1,000 mg/kg)-induced sleep (~2 min, similar to that in GHB 1,000 mg/kg only group). Consistent with the results from the GHB 1,000 mg/kg study, the total sleep time induced by 400 mg/kg GHB, which was calculated as the difference between the time points at the return and loss of righting reflex in rats, was significantly decreased in the 10 mg/kg luteolin treated rats (p<0.05, 60±2 min and 41±12 min for control and luteolin 10 mg/kg groups, respectively). When the AUC of GHB was plotted against GHB-induced total sleep time, a good correlation between these two parameters was observed with a R^2 value of 0.915 (Fig. 3), indicating the total sleep time in rats was closely related to the total exposure of GHB in the plasma. At the return of righting reflex time point, there was no significant difference in GHB plasma concentrations among all control and treatment groups (~0.3 to 0.4 mg/ml, estimated from the data in Fig. 2).

Model Fitting for GHB Pharmacokinetics in the Presence of Luteolin

To further understand the *in vivo* luteolin-GHB interaction, model fitting was used to explore the possible inhibition mechanism. A number of pharmacokinetic models (e.g., a one-, two- or three-compartment model with linear or nonlinear elimination) were first constructed to describe luteolin kinetics. Based on the fitting criteria (e.g., CV % of the estimates, R^2 and AIC), a two-compartment model with linear elimination best characterized luteolin pharmacokinetics (data not shown). The final fitted pharmacokinetic parameters for luteolin were 0.124 min^{-1} (CV %: 16.4), 0.120 min^{-1} (CV %: 17.3), 0.0224 min^{-1} (CV %: 12.2) and 204 ml/kg (CV %: 20.0) for k_{10}, k_{12}, k_{21} and V_{C_Lut}, respectively. Using the selected luteolin model as a base model, an integrated pharmacokinetic model (Fig. 4) was proposed to describe the interaction between luteolin and GHB by incorporating a one-compartment GHB model with capacity-limited metabolism, glomerular filtration, and capacity-limited reabsorption. The parameters of GHB capacity-limited metabolism and glomerular filtration in rats have been previously determined (20) and were fixed in the model fitting (Table 2). In the inhibition model, luteolin was assumed not to inhibit GHB metabolism but to inhibit GHB renal reabsorption via different mechanisms, e.g., competitive, noncompetitive or uncompetitive inhibition (Eqs. 4, 5 and 6). Simultaneous fitting was conducted to compare the goodness-of-fit of these models. Based on the fitting criteria (e.g., CV % of the estimates, R^2, AIC and SC), an uncompetitive inhibition

Table 1. Effects of Luteolin on the Pharmacokinetics and Pharmacodynamics of GHB in Rats

Parameters	GHB (1,000 mg/kg, i.v.)			GHB (400 mg/kg, i.v.)	
	Control (n=6)	Luteolin (4 mg/kg) (n=5)	Luteolin (10 mg/kg) (n=4)	Control (n=4)	Luteolin (10 mg/kg) (n=3)
AUC (mg ml^{-1} min)	170±40	117±29*	113±21*	56.6±6.3	46.6±6.6
Cl (ml min^{-1} kg^{-1})	6.19±1.59	8.92±2.02*	9.05±1.43*	7.13±0.73	8.70±1.33
Urinary recovery %	27.1±9.0	29.9±19.6	42.1±10.3	8.77±4.64	10.9±3.4
Cl_R (ml min^{-1} kg^{-1})	1.64±0.62	2.46±1.31	3.84±1.21*	0.63±0.36	0.93±0.22
Cl_m (ml min^{-1} kg^{-1})	4.55±1.36	6.46±2.85	5.22±1.19	6.50±0.70	7.77±1.37
Sleep Time (min)	161±16	131±14**	121±5**	60±2	41±12*

*p<0.05, compared with the corresponding control group
**p<0.01, compared with the corresponding control group

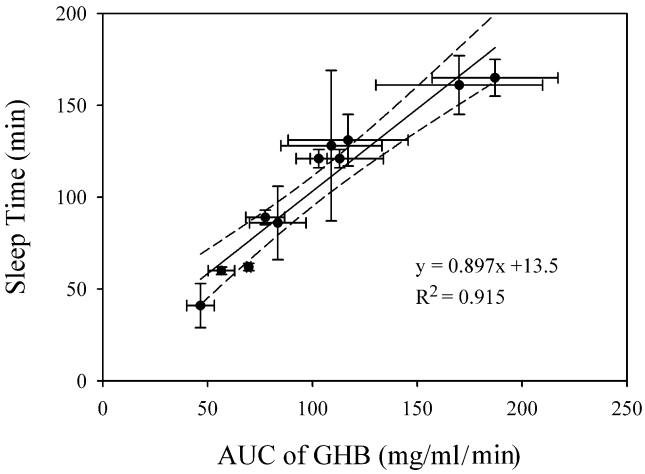

Fig. 3. Concentration–effect relationship for GHB. AUC of GHB (*x*-axis) is plotted against GHB-induced sleep time (*y*-axis). Data are presented as mean ± SD, n=3-6 for each data point. Some of the data in the figure were obtained from a previous study (9), or from unpublished studies (Wang X, Wang Q and Morris ME). The doses of GHB are 400 and 1,000 mg/kg. The *solid line* represents the linear regression of the data. The *dashed lines* represent the 95% confidence intervals

model gave the best fitting results (Table 2). The model fitted data captured well the experimental data (Figs. 1 and 2). The fitted pharmacokinetic parameters of GHB in the final model were 49.2 mg min^{-1} kg^{-1}, 5.54 mg/ml, 578 ml/kg, and 63.3 μg/kg for V_{max_ren}, k_{ren}, V_{GHB}, and K_i, respectively.

Model Simulation for Luteolin and GHB Pharmacokinetic Interaction

To determine the effects of varying doses of luteolin on GHB detoxification at different dose levels of GHB, model simulations were conducted using the parameters obtained from the above nonlinear regression analysis with the incorporation of a 10% variance using ADAPT II software. GHB was given by iv bolus at three hypothesized doses (200, 400 and 1,000 mg/kg) and luteolin was given by iv bolus at five hypothesized doses (0, 2, 4, 10, and 20 mg/kg). As shown in Table 3, the simulation results indicated that luteolin significantly decreased the AUC of GHB and increased the clearance of GHB. The changes were more evident at a higher dose of GHB (1,000 mg/kg) than at a lower dose of GHB (200 mg/kg). For example, at the dose of 10 mg/kg, luteolin decreased the AUC of GHB by approximately 20, 30 and 40% for GHB doses of 200, 400 and 1,000 mg/kg, respectively.

DISCUSSION

Flavonoid-drug interactions with favorable or adverse effects have increasingly been observed in recent years, due to the widespread use of flavonoid-enriched dietary supplements and herbal medicines in the general population for disease prevention and treatment (28–30). The mechanisms underlying most of these interactions are effects (inhibition/induction) on drug metabolizing enzymes and/or efflux drug transporters, such as P-glycoprotein and BCRP (11–13). Limited information is available concerning interactions between flavonoids and uptake transporters. In a previous study, we found that flavonoids represent a class of potent inhibitors of monocarboxylate transporter-1 (MCT1) (9), an uptake transporter important in the transport of endogenous monocarboxylates as well as clinically important drugs (1,5). Therefore, the objectives of this study were to further characterize the flavonoid-drug interactions mediated by MCT1 using GHB as a model substrate, and to explore the possible *in vivo* inhibition mechanism using pharmacokinetic model fitting methods.

The flavonoid luteolin is a potent MCT1 inhibitor, with an IC_{50} of 0.41 μM in inhibiting the uptake of GHB in rat MCT1-transfected MDA-MB231 cells (9). In the present study, the plasma concentrations of luteolin in rats after an intravenous dose of 10 mg/kg are well above 0.41 μM (0.12 μg/ml). At a dose of 4 mg/kg, the plasma concentrations of luteolin are significantly higher than 1 μM (~0.3 μg/ml) for the first 60 min, and remain above 0.36 μM (~0.1 μg/ml) at later time points (Fig. 1), indicating in vivo MCT1 inhibition by luteolin is likely to occur under our experimental conditions.

In this study, GHB was selected as a model MCT1 substrate. Previous studies have demonstrated that *in vivo* GHB elimination following intravenous administration is due to capacity-limited metabolism and capacity-limited renal

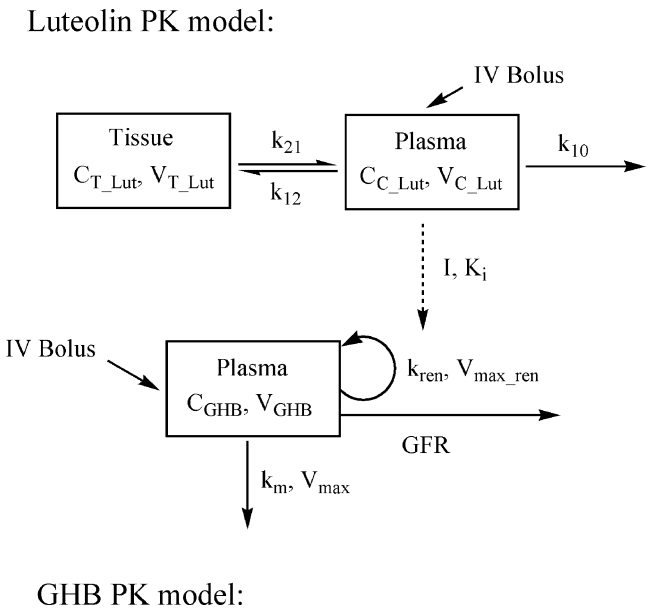

Fig. 4. Proposed model for luteolin and GHB pharmacokinetics. C_{C_Lut} and C_{T_Lut} represent luteolin concentrations in the central and peripheral compartments, respectively. V_{C_Lut} and V_{T_Lut} represent the volume of distribution of luteolin in the central and peripheral compartments, respectively. C_{GHB} and V_{GHB} represent GHB plasma concentration and volume of distribution, respectively. k_{10} represents the luteolin elimination rate constant of the central compartment. k_{12} and k_{21} represent the luteolin first-order distribution rate constants between the central and peripheral compartments. V_{max} represents the maximal metabolic rate of GHB and k_m represents the concentration of GHB at 50% of the maximal metabolic rate. GFR represents the glomerular filtration rate in the kidney. V_{max_ren} represented the maximal renal reabsorption rate of GHB and k_{ren} represents the concentration of GHB at 50% of the maximal reabsorption rate. I represents luteolin in the central compartment that inhibits GHB reabsorption and K_i represents the inhibition constant for 50% inhibition

Table 2. Fitted Pharmacokinetic Parameters from the Integrated GHB and Luteolin Model

	Competitive		Noncompetitive		Uncompetitive	
	Fitted Values	CV %	Fitted Values	CV %	Fitted Values	CV %
V_{max} (mg min^{-1} kg^{-1})	2.27	Fixed	2.27	Fixed	2.27	Fixed
k_m (mg/ml)	0.063	Fixed	0.063	Fixed	0.063	Fixed
V_{GHB} (ml/kg)	567	4.20	563	4.12	578	3.63
GFR (ml min^{-1} kg^{-1})	10	Fixed	10	Fixed	10	Fixed
V_{max_ren} (mg min^{-1} kg^{-1})	24.8	36.2	21.0	28.3	49.2	38.5
k_{ren} (mg/ml)	2.56	44.7	2.05	36.0	5.54	43.5
K_i (μg/kg)	572	20.7	686	17.5	63.3	35.2
AIC	−117		−122		−141	
SC	−104		−109		−127	

clearance (19,20). In the kidney, GHB is extensively reabsorbed from urine into blood (20) and this process is mediated by a family of monocarboxylate transporters. In studies using rat kidney membrane vesicles and human kidney HK-2 cells, MCT1 and MCT2 have been shown as important transporters responsible for GHB renal reabsorption (14,31). However, the contribution of MCT2 in the overall GHB renal transport in HK-2 cells is minor when compared to that of MCT1 (31). Moreover, a single transport process for GHB was observed in rat kidney membrane vesicles based on an Eadie–Hofstee plot, and similar transport kinetic parameters of GHB were obtained from both rat kidney membrane vesicles and rat MCT1-transfected cells (14). Therefore, MCT1 appears to represent a major, if not the only, transporter governing GHB renal reabsorption. Future studies are needed to better characterize the contribution of MCT1 and/or other MCTs to GHB renal reabsorption.

Given the potent MCT1 inhibition activity of luteolin and the significant contribution of MCT1 in GHB renal reabsorption, it is likely that the interaction of luteolin with MCT1 might have significant effects on GHB pharmacokinetics. This hypothesis was tested in a previous report (9) and is confirmed and further characterized in this study. As shown in Fig. 2 and Table 1, luteolin (4 and 10 mg/kg) significantly decreased GHB (1000 mg/kg) plasma concentrations and AUC. At the dose of 10 mg/kg, luteolin significantly increased the total and renal clearances of GHB (1,000 mg/kg) by about 1.5-fold and twofold, respectively. The contribution of renal clearance of GHB to its total clearance was increased from 27% in the control group to 42% in the luteolin 10 mg/kg treatment group. Similarly, luteolin at the dose of 4 mg/kg increased the total and renal clearances of GHB (1,000 mg/kg), although a statistically significant increase was only observed in the total clearance. This is possibly due to the different concentrations of luteolin and the duration of luteolin exposure above the IC_{50} values in two luteolin dose groups. Alternatively, it might be due to the variability in urinary data, requiring a larger sample size to detect statistically significant differences in the renal clearance of GHB following the administration of 4 mg/kg luteolin**.** Interestingly, luteolin had no significant effects on the metabolic clearance of GHB. All these results clearly indicated that luteolin altered GHB pharmacokinetics via increasing GHB renal clearance, which is consistent with the inhibition of MCT1-mediated renal reabsorption. To our knowledge, there is no report of luteolin affecting the metabolism of GHB, which is in agreement with the lack of changes observed in GHB metabolic clearance when determined with or without luteolin treatment. Moreover, it is recognized that GHB metabolism following a 1,000 mg/kg dose is saturated (Table 1) (20) and, as a result, changes in renal clearance might be more readily detected upon treatment with luteolin. At a lower GHB dose level (400 mg/kg), luteolin treatment increased the total and renal clearances of GHB, although the changes were not statistically significant (Table 1). The less pronounced effect at a lower GHB dose is probably due to the nonlinearity in GHB metabolic clearance. At lower doses, GHB metabolism is not saturated, and most GHB (~90%) is eliminated via metabolic transformation (Table 1). Consistent with previous studies,

Table 3. Model Simulation of the Luteolin-GHB Interaction Following i.v. Bolus Doses of GHB and Luteolin in Rats

	GHB (200 mg/kg, i.v. bolus)		GHB (400 mg/kg, i.v. bolus)		GHB (1,000 mg/kg, i.v. bolus)	
Luteolin (i.v. bolus)	AUC (mg ml^{-1} min)	Cl (ml min^{-1} kg^{-1})	AUC (mg ml^{-1} min)	Cl (ml min^{-1} kg^{-1})	AUC (mg ml^{-1} min)	Cl (ml min^{-1} kg^{-1})
0 mg/kg	17.8±3.7	11.6±2.2	52.0±6.0	7.78±0.85	184±9	5.45±0.28
2 mg/kg	16.0±3.3	12.9±2.4	44.0±5.2**	9.20±1.03*	146±8**	6.88±0.38**
4 mg/kg	15.2±3.1	13.6±2.5	40.8±4.8**	9.91±1.10**	132±7**	7.62±0.42**
10 mg/kg	14.0±2.8	14.7±2.7	36.2±4.2**	11.2±1.2**	113±6**	8.91±0.48**
20 mg/kg	13.1±2.5*	15.7±2.8**	32.9±3.7**	12.3±1.3**	100±5**	10.0±0.5**

*$p<0.05$, compared with the corresponding luteolin 0 mg/kg group
**$p<0.01$, compared with the corresponding luteolin 0 mg/kg group

the contribution of GHB renal clearance is less significant at lower GHB doses (20), and therefore, the effects of luteolin on GHB clearance are smaller in magnitude.

Consistent with the effects on GHB pharmacokinetics, luteolin also significantly decreased the GHB-induced total sleep time in rats. The AUC of GHB correlated well with GHB-induced sleep time (Fig. 3, R^2=0.915), indicating the hypnotic effects of GHB are directly related to the plasma concentration of GHB. Interestingly, luteolin (10 mg/kg) significantly delayed the loss of righting reflex induced by 400 mg/kg GHB (10±4 vs 23±8 min for the control and treatment group, respectively), with no effects on the loss of righting reflex induced by 1,000 mg/kg GHB (~2 min for both control and treatment group). This is likely due to the higher concentrations of luteolin at early time points that can affect renal reabsorption and possibly inhibit MCT1-mediated brain uptake (32). This inhibition could be more readily achieved at a relatively lower GHB dose. At the return of righting reflex time point, there was no significant difference in GHB plasma concentrations among all control and treatment groups (~0.3 to 0.4 mg/ml, estimated from the data in Fig. 2), indicating this concentration might represent the wake-up threshold concentration in rats.

To better understand the interaction between luteolin and GHB, an integrated pharmacokinetic model was constructed to describe the *in vivo* data. First of all, luteolin pharmacokinetics was determined based on the fitting results from different models (data not shown). A two-compartment linear model provides the best fit, which is consistent with literature reports of other flavonoid analogues, such as quercetin (33) and puerarin (34). In addition, the dose-proportional AUC and constant clearance at different luteolin doses in this study further supported the linear kinetics of luteolin. As for the pharmacokinetics of GHB, a one-compartment model was selected with the incorporation of capacity-limited metabolism, glomerular filtration, and capacity-limited reabsorption, according to the previous reports (19,20). In this model, we assumed MCT1 represented the major player determining GHB renal reabsorption, based on the results in HK-2 cells and the observed single transport process of GHB in rat kidney membrane vesicles (14,31).

The final fitting results from the integrated model showed that the uncompetitive inhibition model gave the best fitting, with an AIC value of –141. This is consistent with several other studies, in which luteolin has been reported as an uncompetitive inhibitor of N-acetyltransferase (35) and tyrosinase (36). However, this result differs from our previous *in vitro* study showing that luteolin competitively inhibited GHB uptake into MDA-MB231 cells (9). In our *in vitro* study, only one luteolin concentration (50 μM) was used to discern the inhibition kinetics (9). Further studies are needed to evaluate the inhibition mechanism. As shown in Figs. 1 and 2, the fitted results captured well the experimental data with small CV % values (Table 2), indicating that the proposed model reasonably described the *in vivo* interaction. The value of V_{GHB} determined in this study was very close to a previous reported value (19). The Ki value determined is 63.3 μg/kg, which is an apparent value. Using the luteolin volume of distribution (204 ml/kg), the true Ki value will be around 1.1 μM, which is close to the *in vitro* IC_{50} value (0.41 μM). If we consider the contribution of protein binding of luteolin in plasma, the true Ki value will be even smaller. In a previous study, the free fraction (fu) of quercetin, an analogue of luteolin, in plasma has been reported around 1% (37). Therefore, if we assume the similar protein binding of quercetin and luteolin, the true Ki value determined *in vivo* will be close to 0.01 μM ($Ki \cdot fu/V_{C\_LUT}$), indicating luteolin is a more potent MCT1 inhibitor *in vivo* comparing to its in vitro inhibition. In a previous study, the protein binding of GHB was reported to be negligible (20). Therefore, the GHB concentrations determined in the study (total concentration) also represent the unbound concentrations of GHB in the plasma.

In the model simulations using the parameters obtained from model fitting, luteolin was shown to significantly decrease the AUC of GHB and increase the clearance of GHB. The changes were more evident at higher doses of GHB (1,000 mg/kg) than at lower doses of GHB (200 mg/kg). This is possibly due to the more significant contribution of GHB renal clearance to the total clearance, when metabolic clearance is saturated.

CONCLUSION

The results of this study characterized the effects of the flavonoid luteolin on GHB pharmacokinetics and pharmacodynamics. The pharmacokinetic interaction was well described by an uncompetitive inhibition model consisting of capacity-limited metabolic clearance and capacity-limited renal clearance. Inhibiting MCT1 by the flavonoid luteolin might represent a potential mechanism for GHB detoxification following overdoses of GHB.

ACKNOWLEDGMENTS

This work was funded by NIH Grant DA14988. We would like to thank Ms. Sunmi Fung for her excellent assistance in LC/MS/MS analysis.

REFERENCES

1. A. P. Halestrap, D. Meredith. The SLC16 gene family-from monocarboxylate transporters (MCTs) to aromatic amino acid transporters and beyond. *Pflugers Arch.* **447**(5)619–628 (2004).
2. A. P. Halestrap, N. T. Price. The proton-linked monocarboxylate transporter (MCT) family: structure, function and regulation. *Biochem. J.* **343**(Pt 2)281–299(1999).
3. I. Tamai, Y. Sai, A. Ono, Y. Kido, H. Yabuuchi, H. Takanaga, E. Satoh, T. Ogihara, O. Amano, S. Izeki, A. Tsuji. Immunohistochemical and functional characterization of pH-dependent intestinal absorption of weak organic acids by the monocarboxylic acid transporter MCT1. *J. Pharm. Pharmacol.* **51**(10)1113–11211999.
4. A. Okamura, A. Emoto, N. Koyabu, H. Ohtani, Y. Sawada. Transport and uptake of nateglinide in Caco-2 cells and its inhibitory effect on human monocarboxylate transporter MCT1. *Br. J. Pharmacol.* **137**(3)391–399 (2002).
5. K. Nagasawa, K. Nagai, Y. Sumitani, Y. Moriya, Y. Muraki, K. Takara, N. Ohnishi, T. Yokoyama, S. Fujimoto. Monocarboxylate transporter mediates uptake of lovastatin acid in rat cultured mesangial cells. *J. Pharm. Sci.* **91**(12)2605–2613 (2002).

6. C. Manach, A. Scalbert, C. Morand, C. Remesy, L. Jimenez. Polyphenols: food sources and bioavailability. *Am. J. Clin. Nutr.* **79**(5)727–747 (2004).
7. K. Horvathova, L. Novotny, D. Tothova, A. Vachalkova. Determination of free radical scavenging activity of quercetin, rutin, luteolin and apigenin in H2O2-treated human ML cells K562. *Neoplasma.* **51**(5)395–399 (2004).
8. A. Kotanidou, A. Xagorari, E. Bagli, P. Kitsanta, T. Fotsis, A. Papapetropoulos, C. Roussos. Luteolin reduces lipopolysaccharide-induced lethal toxicity and expression of proinflammatory molecules in mice. *Am. J. Respir. Crit. Care Med.* **165**(6)818–823 (2002).
9. Q. Wang, M. E. Morris. Flavonoids modulate monocarboxylate transporter-1-mediated transport of gamma-hydroxybutyrate *in vitro* and *in vivo*. *Drug Metab. Dispos.* **35**(2)201–208 (2007).
10. G. K. Dresser, D. G. Bailey, B. F. Leake, U. I. Schwarz, P. A. Dawson, D. J. Freeman, R. B. Kim. Fruit juices inhibit organic anion transporting polypeptide-mediated drug uptake to decrease the oral availability of fexofenadine. *Clin. Pharmacol. Ther.* **71**(1)11–20 (2002).
11. J. S. Choi, H. K. Choi, S. C. Shin. Enhanced bioavailability of paclitaxel after oral coadministration with flavone in rats. *Int. J. Pharm.* **275**(1–2)165–170 (2004).
12. Y. H. Wang, P. D. Chao, S. L. Hsiu, K. C. Wen, Y. C.Hou. Lethal quercetin-digoxin interaction in pigs. *Life Sci.* **74**(10)1191–1197 (2004).
13. X. Wang, M. E. Morris. Effects of the flavonoid chrysin on nitrofurantoin pharmacokinetics in rats: Potential involvement of ABCG2. *Drug Metab. Dispos.* **35**(2)268–274 (2007).
14. Q. Wang, I. M. Darling, M. E. Morris. Transport of gamma-hydroxybutyrate in rat kidney membrane vesicles: Role of monocarboxylate transporters *J. Pharmacol. Exp. Ther.* **318**(2) 751–761 (2006).
15. M. Mamelak, M. B. Scharf, M. Woods. Treatment of narcolepsy with gamma-hydroxybutyrate. A review of clinical and sleep laboratory findings. *Sleep*. **9**(1 Pt 2)285–289 (1986).
16. K. R. Drasbek, J. Christensen, K. Jensen. Gamma-hydroxybutyrate–a drug of abuse. *Acta Neurol. Scand*. **114**(3)145–156 (2006).
17. P. E. Mason, W. P. Kerns 2nd. Gamma hydroxybutyric acid (GHB) intoxication. *Acad Emerg. Med.* **9**(7)730–739 (2002).
18. J. Lettieri, H. L. Fung. Absorption and first-pass metabolism of 14C-gamma-hydroxybutyric acid. *Res. Commun. Chem. Pathol. Pharmacol*. **13**(3)425–437 (1976).
19. J. T. Lettieri, H. L. Fung. Dose-dependent pharmacokinetics and hypnotic effects of sodium gamma-hydroxybutyrate in the rat. *J. Pharmacol. Exp. Ther.* **208**(1)7–11 (1979).
20. M. E. Morris, K. Hu, Q. Wang. Renal clearance of gamma-hydroxybutyric acid in rats: increasing renal elimination as a detoxification strategy. *J. Pharmacol. Exp. Ther.* **313**(3)1194–1202 (2005).
21. P. Palatini, L. Tedeschi, G. Frison, R. Padrini, R. Zordan, R. Orlando, L. Gallimberti, G. L. Gessa, S. D. Ferrara. Dose-dependent absorption and elimination of gamma-hydroxybutyric acid in healthy volunteers. *Eur. J. Clin. Pharmacol.* **45**(4)353–356 (1993).
22. C. Arena, H. L. Fung. Absorption of sodium gamma-hydroxybutyrate and its prodrug gamma-butyrolactone: relationship between *in vitro* transport and *in vivo* absorption. *J. Pharm. Sci*. **69**(3)356–358 (1980).
23. L. Li, H. Jiang, H. Wu, S. Zeng. Simultaneous determination of luteolin and apigenin in dog plasma by RP-HPLC. *J. Pharm. Biomed. Anal*. **37**(3)615–620 (2005).
24. T. Chen, L. P. Li, X. Y. Lu, H. D. Jiang, S. Zeng. Absorption and excretion of luteolin and apigenin in rats after oral administration of Chrysanthemum morifolium extract. *J. Agric. Food Chem.* **55**(2)273–277 (2007).
25. H. L. Fung, E. Haas, J. Raybon, J. Xu, S. M. Fung. Liquid chromatographic-mass spectrometric determination of endogenous gamma-hydroxybutyrate concentrations in rat brain regions and plasma. *J. Chromatogr. B Analyt. Technol. Biomed. Life Sci.* **807**(2)287–291 (2004).
26. B. Ferrier, M. Martin, B. Janbon, G. Baverel. Transport of beta-hydroxybutyrate and acetoacetate along rat nephrons: A micropuncture study. *Am. J. Physiol*. **262**(5 Pt 2)F762–769 (1992).
27. D. K. Van Sassenbroeck, P. De Paepe, F. M. Belpaire, W. A. Buylaert. Characterization of the pharmacokinetic and pharmacodynamic interaction between gamma-hydroxybutyrate and ethanol in the rat. *Toxicol. Sci.* **73**(2)270–278 (2003).
28. B. H. Havsteen.The biochemistry and medical significance of the flavonoids. *Pharmacol. Ther.* **96**2–367–202 (2002).
29. C. M. Kruijtzer, J. H. Beijnen, H. Rosing, W. W. ten Bokkel Huinink, M. Schot, R. C. Jewell, E. M. Paul, J. H. Schellens. Increased oral bioavailability of topotecan in combination with the breast cancer resistance protein and P-glycoprotein inhibitor GF120918. *J. Clin. Oncol*. **20**(13)2943–2950 (2002).
30. A. Sparreboom, M. C. Cox, M. R. Acharya, W. D. Figg. Herbal remedies in the United States: Potential adverse interactions with anticancer agents. *J. Clin. Oncol*. **22**(12)2489–2503 (2004).
31. Q. Wang, Y. Lu, M. E. Morris. Monocarboxylate transporter (MCT) mediates the transport of gamma-hydroxybutyrate in human kidney HK-2 cells. *Pharm. Res*. **24**(6)1067–1078 (2007).
32. I. Bhattacharya, K. M. Boje. GHB (gamma-hydroxybutyrate) carrier-mediated transport across the blood-brain barrier. *J. Pharmacol. Exp. Ther.* **311**(1)92–98 (2004).
33. D. R. Ferry, A. Smith, J. Malkhandi, D. W. Fyfe, P. G. deTakats, D. Anderson, J. Baker, D. J. Kerr. Phase I clinical trial of the flavonoid quercetin: Pharmacokinetics and evidence for in vivo tyrosine kinase inhibition. *Clin. Cancer Res*. **2**(4)659–668 (1996).
34. Y. Li, W. S. Pan, S. L. Chen, H. X. Xu, D. J. Yang, A. S. Chan. Pharmacokinetic, tissue distribution, and excretion of puerarin and puerarin-phospholipid complex in rats. *Drug Dev. Ind. Pharm*. **32**(4)413–422 (2006).
35. Y. C. Li, C. F. Hung, F. T. Yeh, J. P. Lin, J. G. Chung. Luteolin-inhibited arylamine N-acetyltransferase activity and DNA-2-aminofluorene adduct in human and mouse leukemia cells. *Food Chem. Toxicol.* **39**(7)641–647 (2001).
36. L. P. Xie, Q. X. Chen, H. Huang, H. Z. Wang, R. Q. Zhang. Inhibitory effects of some flavonoids on the activity of mushroom tyrosinase. *Biochemistry (Mosc)*. **68**(4)487–491 (2003).
37. D. W. Boulton, U. K. Walle, T. Walle. Extensive binding of the bioflavonoid quercetin to human plasma proteins. *J. Pharm. Pharmacol*. **50**(2)243–249 (1998).